5.5

Deep Convection

John Lazier, Robert Pickart and Peter Rhines

5.5.1 Convection and spreading

Density of ocean water generally increases with depth. At the surface, however, stirring by waves and convection creates a well-mixed homogeneous layer. Waves alone can mix the upper ≈50–100 m. But convection, forced by an increase in density at the surface via heat loss or evaporation, can greatly increase the mixed-layer depth. During winter, heat loss from the surface of the ocean is high and convectively mixed surface layers are the norm in the extratropical oceans. The deepest (>1500 m) are found in the Labrador Sea (Fig. 5.5.1), the Greenland Sea (see Dickson *et al.*, Chapter 7.3) and the Golfe du Lion in the Mediterranean Sea (see Candela, Chapter 5.7), because of two unique features. First, they are near land where cold air flows over the water to create the necessary high heat loss. And second, they have weak cyclonic circulations, which keeps the convecting water confined and relatively stationary where the high heat loss occurs. This combination provides the persistent heat loss from the same body of water that is needed to force convection to reach great depths.

An example of a layer mixed by convection is illustrated in Figure 5.5.2 by a plot of $\sigma_{1.5}$ ($\sigma_{1.5}$ + 1000 = potential density in kg m^{-3} referenced to 1500 decibars (1 decibar corresponding to about 1 m)) versus depth, on 25 February and 8 March, in the Labrador Sea. The convective layer is the approximately homogeneous layer next to the surface about 750 m deep with a $\sigma_{1.5}$ of 34.652 kg m^{-3} on 25 February (Station 66) and 1150 m deep and 34.673 kg m^{-3} 11 days later (Station 118). In the potential temperature versus salinity plots of these two stations (Fig. 5.5.3) the homogeneous layer is identified by the concentrations of temperature and salinity values next to the station labels. Beneath this upper layer temperature and salinity both increase well above the values observed in the mixed layer. At Station 66, for instance, the temperature and salinity in the mixed layer are 2.82°C and 34.806 down to ≈700 m but 3.02°C and 34.845 at 750 m. As deepening of the mixed layer continues it mixes into and incorporates this warmer, saltier water, which increases the salinity of the mixing layer. This explains why the salinity in the mixing layer is higher at Station 118 than at Station 66 (Fig. 5.5.3). The heat added from the warm water below also increases the temperature of the mixing layer. In this case the value at Station 118 is not above that at Station 66, but it is above the value it would have been without the extra heat from below.

A common relationship studied in deep convection regions is that between heat loss from the surface and the resulting depth of convection. A simple way of estimating this is to integrate the buoyancy between the existing and final conditions and convert the integrated buoyancy loss to a heat loss. For example, in the situation shown in Fig. 5.5.2, it is of interest to know how much heat loss is required to increase the density of the mixed layer to 1034.694 kg m^{-3} ($\sigma_{1.5}$ = 34.694) which occurs at ≈2000 m. The change of slope at this depth in the curve in Fig. 5.5.2 indicates the greatest depth reached by convection during the severe winters of 1993 and 1994. Starting with

OCEAN CIRCULATION AND CLIMATE
ISBN 0-12-641351-7

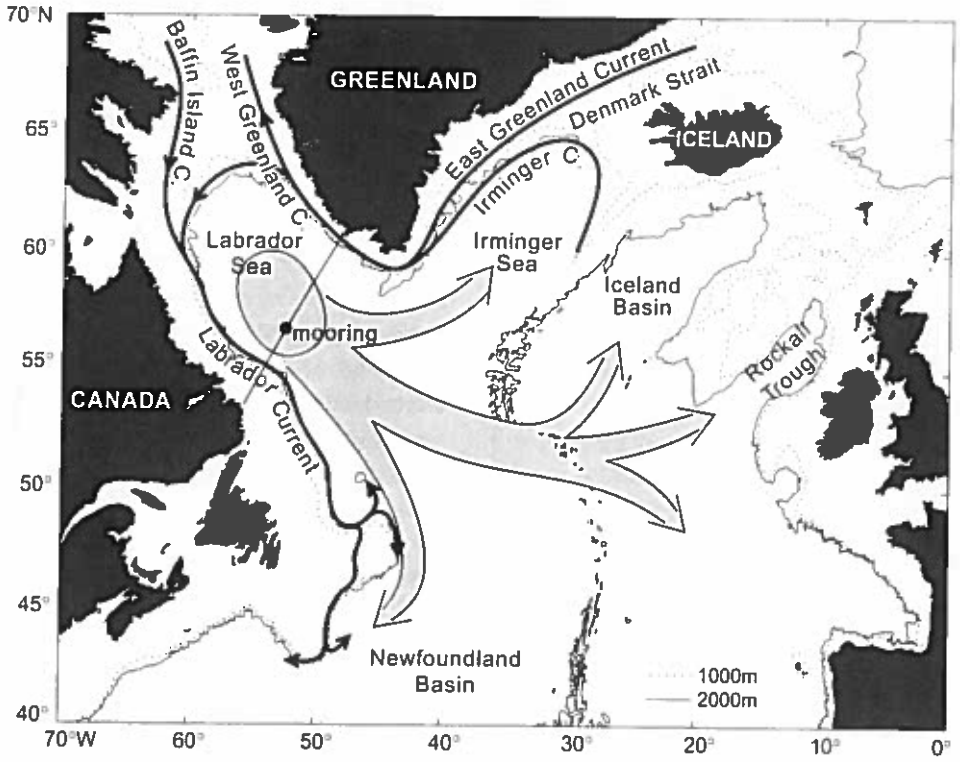

Fig. 5.5.1 Map of the northern North Atlantic showing the Labrador, Greenland and Irminger Currents, which border or influence the Labrador Sea. The WOCE AR7W CTD line across the Labrador Sea and the *Bravo* mooring on the line are indicated by a line and dot. The flows of the intermediate depth Labrador Sea Water (LSW) away from the Labrador Sea eastward to the Irminger Sea and the eastern North Atlantic, and southward to Newfoundland Basin are indicated by the broad open arrows. Adapted from Sy *et al.* (1997).

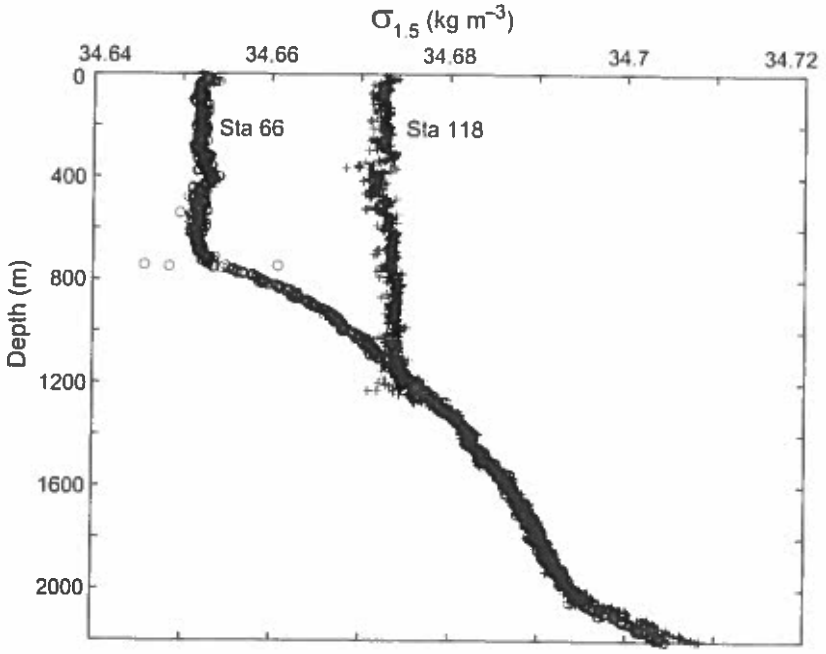

Fig. 5.5.2 Vertical distribution of σ_{15} obtained from Research Vessel (RV) *Knorr* at 56.8°N 54.2°W in the Labrador Sea on 25 February (Station 66) and 8 March 1997 (Station 118).

the observations at Station 66 the required buoyancy loss is found by calculating

$$g/\rho_0 \int \Delta\rho \, dz$$

where g (10 m s^{-2}) is the acceleration due to gravity, ρ_0 ($\approx$1034 kg m^{-3}) is the reference density, z is the depth and $\Delta\rho$ is the difference in density between Station 66 and a density of 1034.694 kg m^{-3}. This yields a buoyancy loss of 0.47 m^2 s^{-2}, which can be converted to joules by dividing by $g\alpha/\rho_0 c$ where g and ρ_0 are as before, α (10^{-4} °C^{-1}) is the thermal expansion of water and c (4.2 kJ kg^{-1} °C^{-1}) is the specific heat capacity of seawater. The conversion suggests a heat loss of $\approx 2 \times 10^9$ J m^{-2} will create a mixed layer to 2000 m and density of 1034.694 kg m^{-3}. Since Station 66 was obtained on 25 February, only 35 days before the usual end of the cooling season on 1 April, it would require a heat flux of about 630 W m^{-2} over the 35 days. Although such high heat fluxes have been observed in the area (see The Lab Sea Group, 1998), they are relatively rare and only sustained for significant periods in exceptionally severe winters.

A similar buoyancy calculation starting with data obtained near the end of summer in 1996 yields $\approx 4 \times 10^9$ J m^{-2} as the heat loss required to create a convection layer to 2000 m or 1034.694 kg m^{-3}. Over the approximately 180 days of cooling between 1 October and 1 April this would require an average heat flux of $\approx$250 W m^{-2}. Smith and Dobson (1984) calculated that between October and April the average heat loss from the central Labrador Sea, based on meteorological observations at Ocean Weather Ship *Bravo* (56.5°N 51°W) between 1946 and 1974, is $\approx 150 \pm 60$ W m^{-2}. These values imply that a winter severe enough to produce convection to 2000 m, i.e. $\approx$250 W m^{-2} for 180 days, would occur when the heat loss over the winter was larger than the average by $\approx$1.5 standard deviations or roughly once in 10 years; this is about what is observed.

The buoyancy calculation is also useful because it is dependent only on the density profile. If the density profile remains unchanged, the heat loss required to produce a mixed layer to a given depth remains the same; independent of changes in the temperature and salinity profiles. In the Labrador Sea this point arises with the warmer, saltier water evident beneath the mixed layer in Figure 5.5.3. This water originates in the North Atlantic Current and is carried into the Labrador Sea from the Irminger Sea by the Greenland Currents. Its temperature and salinity vary with time but the density tends to remain roughly constant as the temperature effect on density is largely compensated by an opposite salinity effect. Thus in a given year the temperature and salinity in this layer may be higher than average, but if the density profile is

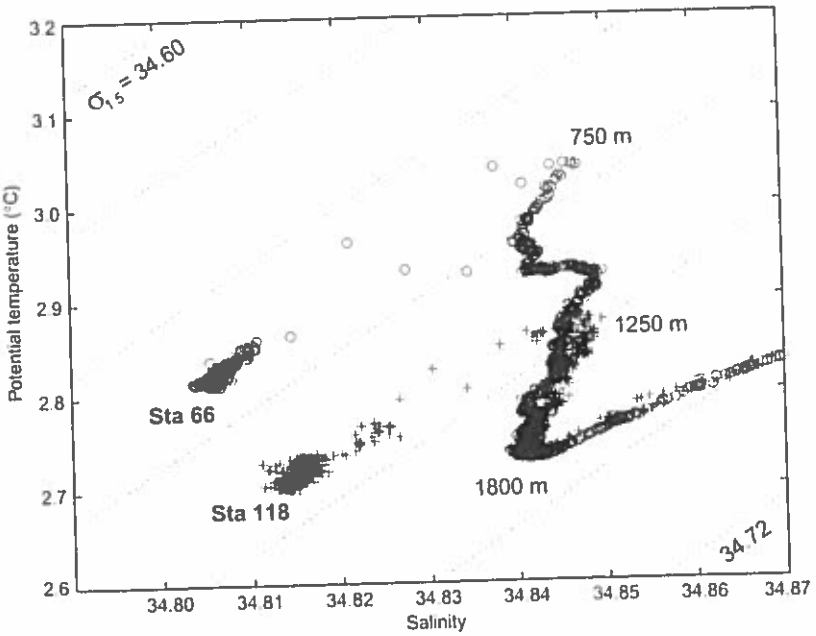

Fig. 5.5.3 Temperature versus salinity distributions at the same stations plotted in Figure 5.5.2. The observations in the mixed surface layers are clustered near the station labels. The sloping dotted lines indicate surfaces of constant $\sigma_{1.5}$.

not changed, the buoyancy is not changed and the depth of convection, for a given heat loss, will not be altered.

The foregoing one-dimensional view of convection is expanded to two dimensions in the contour plot of salinity (Fig. 5.5.4, see Plate 5.5.4, p. 428) obtained in the Labrador Sea in July following the exceptionally cold winter of 1992–93. The water mass resulting from convection is the large volume of homogeneous water lying between 360 and 800 km on the horizontal scale and 500 and 2300 m in the vertical. Because of its large volume and unique temperature and salinity properties that are renewed in the Labrador Sea, the water mass has its own name; the Labrador Sea Water (LSW).

The newly formed Labrador Sea Water is a mixture of all the water down to 2300 m including the water in contact with the atmosphere at the surface. In these uppermost layers the concentration of gases such as oxygen, carbon dioxide, tritium and chlorofluorocarbons (CFCs) are at or near equilibrium with the atmosphere. By transporting these gases down from the upper layers of the ocean to intermediate depths, convection provides a mechanism to ventilate the deeper layers, which is one of the most important consequences of deep convection. Dissolved oxygen, for example, is slowly used up in the deep ocean by biological processes and would eventually vanish without the renewal via convection. Also most of the carbon dioxide ever put in the atmosphere by volcanoes since the formation of the earth became dissolved in the ocean and is now contained in sediments in the bottom of the ocean. As combustion of fossil fuels over the earth raises the carbon dioxide content of the atmosphere it is important to understand the rate this gas is entering the deeper layers of the ocean through processes such as deep convection.

The upper layer (0–500 m) in the central part of the salinity section in Figure 5.5.4 (see Plate 5.5.4, p. 428) is clearly not as well mixed as the layer between 500 and 2300 m. This is because the observations were obtained in July about 3 months after deep convection ceased at the end of the cooling season about 1 April. Since that time the surface layer has been flooded with fresh water derived from melting ice and river runoff. As well, the layer below this low-salinity surface layer, to about 500 m, has been invaded by higher-salinity water from the right, that is, the northeast. This more saline water is the water found under the convection layer in Figure 5.5.3 and is known as the Irminger Water (IW) because it is transported into the Labrador Sea from the Irminger Sea in the East and West Greenland Currents that lie over the continental shelf and slope (Fig. 5.5.1). On the left or southwest part of the section there is again a salinity maximum at about 300 m over the Labrador continental slope, which also tends to invade the central region. This is again Irminger Water, which has been transported around the Labrador Sea in the West Greenland and Labrador Currents. Beneath the LSW, between 2300 and 3300 m, lies a water mass identified by the salinity maximum at about 2800 m. This is the North East Atlantic Deep Water (NEADW). It originates in the eastern basin of the North Atlantic and flows into the western basin through gaps in the Mid-Atlantic Ridge. At the bottom of the section is the Denmark Strait Overflow Water (DSOW) with a slightly lower salinity than in the NEADW above. DSOW is the densest water in the northern North Atlantic; it originates in the seas north of Iceland and comes to the Labrador Sea after flowing over the sill in Denmark Strait between Greenland and Iceland (see Saunders, Chapter 5.6). The last water mass of note in the section is the low-salinity water over the Labrador continental shelf that flows south out of Baffin Bay in the Baffin Island Current and the Labrador Current. A similar band of low-salinity water of Arctic origin lies over the Greenland continental shelf but it was covered by heavy ice in July 1993 and not sampled when the rest of these data were collected. The rapid transition between the low-salinity waters over the shelves and the higher-salinity waters of the sea's interior mark the baroclinic currents lying over the upper part of the continental slopes, i.e. the Labrador and West Greenland Currents.

In the Atlantic Ocean, ventilation of the intermediate layers by deep convection occurs only in the Labrador Sea. The historical notion has been that the overturning occurs primarily in the western interior of the basin. Indeed, this is where it has been observed the most (Clarke and Gascard, 1983; Wallace and Lazier, 1988; Lilly *et al.*, 1999). Recent evidence has demonstrated, however, that convection can (at least on occasion) occur closer to the western boundary, directly into the rim current system (Pickart *et al.*, 2000a). Not surprisingly, this boundary current water mass product is less dense than the interior water mass, and

becomes restratified more quickly. Theoretical considerations suggest that convection adjacent to a sloping boundary should result in a greater net vertical sinking of water than overturning in the interior (Hallberg and Rhines, 1996; Spall and Pickart, 2000).

Subsequent to formation, the new LSW spreads to other regions of the ocean at intermediate depths. Our knowledge of the speed of this flow and its influence increased during the World Ocean Circulation Experiment (WOCE) due to the widespread high quality observations of temperature, salinity and CFCs across the North Atlantic. One study by Sy *et al.* (1997) suggested that the newly ventilated water formed in the Labrador Sea during the severe winters of the early 1990s moved into the Irminger Sea within months, to the Iceland Basin within a year, and to Rockall Trough on the eastern boundary in approximately 5 years, yielding a trans-Atlantic speed of approximately $2\,cm\,s^{-1}$. This speed is about three to four times greater than the previous estimate, and one conclusion is that the intermediate flows are much faster than previously thought. An alternative explanation, however, is that convection occurred over a far greater extent of the Labrador Basin during this high NAO (North Atlantic Oscillation) period. This would allow for more direct (and much faster) contact of the new water with both the North Atlantic Current, and Deep Western Boundary Current (including convection directly into the latter as noted above). In this scenario, the 'initial condition' for escape from the Labrador Sea is greatly enhanced. Regarding the surprisingly short time lag to the Irminger Basin (6 months according to Sy *et al.*, 1997), yet another scenario is possible: that deep convection occurred within the Irminger Basin itself. This possibility is raised by Pickart *et al.* (2000b).

The far-field influence of LSW in the subtropical gyre was examined by Curry *et al.* (1998) in a comparison of six decades of data from the Labrador Sea and from the ocean near Bermuda. A correlation between these two regions suggests the products of deep convection in the Labrador Sea impact the waters off Bermuda after about 6 years. These studies along with others such as those by Cunningham and Haine (1995a,b) confirm the LSW flow patterns mapped by Talley and McCartney (1982) and sketched in Figure 5.5.1.

For the reader wishing a more thorough review of deep convection, Marshall and Schott (1999) provide an excellent summary of studies of observations, laboratory experiments, theory and modelling. Also the Labrador Sea is the focus of two recent descriptions. The first, by the Lab Sea Group (1998), concentrates on the observations obtained in conjunction with the cruise of the *Knorr* to the Labrador Sea in January and February 1997. This includes high-resolution numerical simulations and data from meteorological measurements, CTD surveys and neutrally buoyant floats. The second by Lilly *et al.* (1999) concentrates on the observations obtained from a moored placed in the central part of the sea between 1994 and 1995, and by drifting, profiling P-ALACE (Profiling-Autonomous Lagrangian Circulation Explorer) floats.

In the next section some features of plumes, the convective mixing agents, are reviewed. This is followed in Sections 5.5.3 and 5.5.4 by discussions of two phenomena associated with the convection. The first is the increase in the amplitude of temperature and salinity variability during convection observed in moored records. The second is the restratification of the density field following the cessation of convection.

5.5.2 Plumes – the mixing agent

Convection begins to increase the depth of the mixed layer in the Labrador Sea near the end of September when the surface net buoyancy flux from the surface turns from positive to negative. Deepening continues until about the end of March, when the buoyancy flux again becomes positive. The effect of this deepening on the density structure is illustrated, for part of the water column, by the year-long time series of $\sigma_{1.5}$ at five depths between 260 m and 2000 m plotted in Figure 5.5.5 (see Plate 5.5.5, p. 428). The deepening mixed layer is indicated to have reached the instrument at 260 m by the rapid increase in $\sigma_{1.5}$ in the first week in February. This is followed a week or so later by a similar increase at 510 m as the mixed layer reaches that instrument. The fact that the $\sigma_{1.5}$ at these two depths continues to increase until the end of the first week in March suggests the mixed layer continues to increase in depth and density during this interval. After the first week in March, $\sigma_{1.5}$ at 260 and 510 m remain relatively constant for about 3 weeks. This likely indicates convection is continuing but that the buoyancy

flux is now not great enough to increase noticeably the density and depth of the mixing layer. The end of convection is indicated in these data by the sudden decrease in $\sigma_{1.5}$ at 260 and 510 m at the end of March. This change indicates the beginning of the restratification process, which is discussed more fully in Section 5.5.3.

When convection is active, water at the surface becomes denser than the underlying water and descends in plumes. This water is replaced by slightly lighter water rising toward the surface. The physical features of the convecting water including the plumes and the water between has been the subject of a number of investigations, most notably by the group of scientists at Kiel working in the Golfe du Lion in the Mediterranean Sea with moored Acoustic Doppler Current Profilers (ADCPs) and current meters. The cartoon in Figure 5.5.6 summarizes some of the main features of plumes and the mixing layer as described by Schott and Leaman (1991), Schott *et al.* (1993b, 1996) and Send and Marshall (1995).

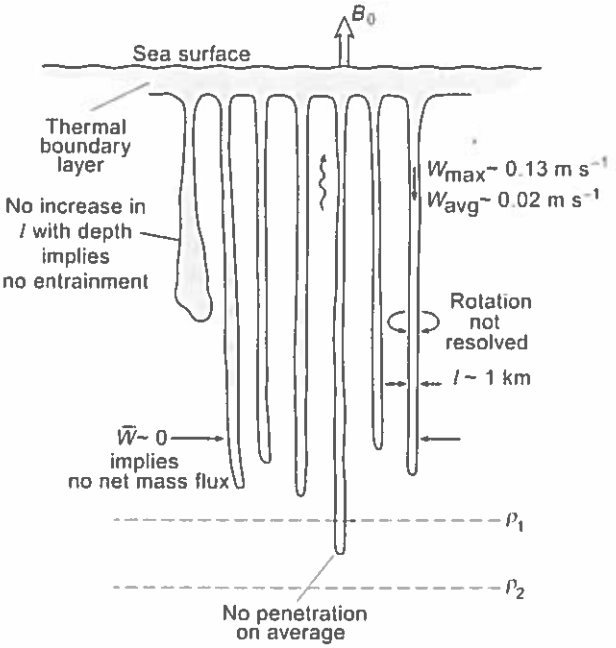

Fig. 5.5.6 Schematic diagram of a convecting layer indicating approximate values for features of individual plumes, including the horizontal scale, vertical downward velocity, rotation and entrainment. Across the patch of convecting water there is no net vertical mass flux and no significant penetration into the layers of denser water beneath the convecting layer. Buoyancy (B_0) lost from the surface creates the thermal boundary layer in the upper $\approx$ 100 m where the denser water that sinks within the plumes is formed. The wiggly up arrow indicates the upward flow (slow) that replaces the downward flow (fast) within the plumes.

At the surface in this picture is the thermal boundary layer where the water is losing heat buoyancy to the atmosphere. Water in this layer is on average, slightly denser than in the mixed layer beneath and descends into the mixing layer within plumes that have a horizontal dimension of $\approx$ 1 km; i.e. an aspect ratio of $\approx$ 1. The average rate of descent within the plumes is $\approx 0.02\,m\,s^{-1}$ while the maximum is $\approx 0.13\,m\,s^{-1}$. Rotation of the plumes, due to the horizontal component of the Coriolis force, is expected because water must converge into the plume at its top and presumably diverge out of it near the bottom. However, this effect has not yet been conclusively observed in the field, although it has been observed in laboratory experiments, e.g. by Helfrich (1994) and Maxworthy and Narimousa (1994), and in numerical simulations, e.g. by Jones and Marshall (1993). Another effect that has not been observed is an increasing horizontal dimension with depth that is expected if water is entrained into the plumes as they descend.

These investigators have also concluded there is no net vertical mass flux within a convecting region or patch. This appears to have solved the long-standing puzzle of whether the descending water was replaced by rising water between the plumes or by converging flow in the upper layer and diverging flow in the deep layer. Finally, they suggest that on average the plumes are not penetrative, that is, the plumes do not have the energy to descend into water that is denser than the water within the plume. One consequence of this is illustrated in Figure 5.5.2 by the fact that the bottom of the mixing layer at Station. 118 lies on the $\sigma_{1.5}$ versus depth curve observed earlier at Station 66. If convection were penetrative the bottom of the mixed layer would lie below this curve and the $\sigma_{1.5}$ versus depth gradient below the mixing layer would be greater than observed earlier, as has been described by Deardorff *et al.* (1969) in tank experiments.

A new and direct view of the motion within convecting plumes has recently been obtained from freely drifting floats (Lab Sea Group, 1998). When a float is launched it immediately sinks to a predetermined depth below the convecting layer where it remains for 7 days while its buoyancy adjusts. At the end of this period its buoyancy decreases slightly and it rises into the convecting

layer. A large attached drogue then pulls the float up and down with the convecting water. In the Labrador Sea over 25 days in February and March 1997 the maximum vertical velocity observed by the floats was downward at $0.2\,m\,s^{-1}$ with a rms value for all the observations of $0.02\,m\,s^{-1}$, suggesting an average round trip for a parcel of 1 day. On a number of occasions the floats were seen to penetrate below the average bottom of the mixing layer. This suggests that, contrary to the conclusions mentioned above that the convection is not penetrative, a certain amount of plume penetration into denser layers does occur. As these floats also record temperature to within 0.001°C it is possible to calculate the vertical heat flux through the mixing layer from the difference in the temperature of the descending water and the ascending water.

5.5.3 Temperature and salinity variability

The previous section discussed some features of convection that are now better understood because of time series records obtained during convection. An additional feature noted in these records is an increase, during convection, in the amplitude of temperature and salinity variability. This was noted by Lilly *et al.* (1999) in records obtained from a mooring in the Labrador Sea (Fig. 5.5.5, see Plate 5.5.5, p. 428). An example of this phenomenon is evident in the temperature record at 510 m in Figure 5.5.7, where the variations in temperature suddenly increase in the middle of February when the deepening mixed layer reaches this depth. Spectra calculated from 85-day pieces of this record before and after the arrival of the convection layer, Figure 5.5.8, show a broadband four-fold increase in the energy of the variability after the sensor is immersed in the mixed layer. A time series (not shown) of this energy, between 0.32 and 0.06 cph, calculated from sequential 256-h blocks of data, shows a peak in February shortly after the mixed layer arrives, followed by a decline to 1/30th of the peak value by the end of the record in June. The minimum energy in the record is in November at a value 1/60th of the peak, which arrives 3 months later. The decline from the beginning of the record to the minimum in November is presumably due to higher energy levels created during convection in the winter prior to the setting of the mooring.

Lilly *et al.* (1999) also demonstrated that the effect of the temperature fluctuations on density were largely compensated by fluctuations in salinity, suggesting that much of the fluctuations are along density surfaces rather than across them. This observation is illustrated in Figure 5.5.9 in

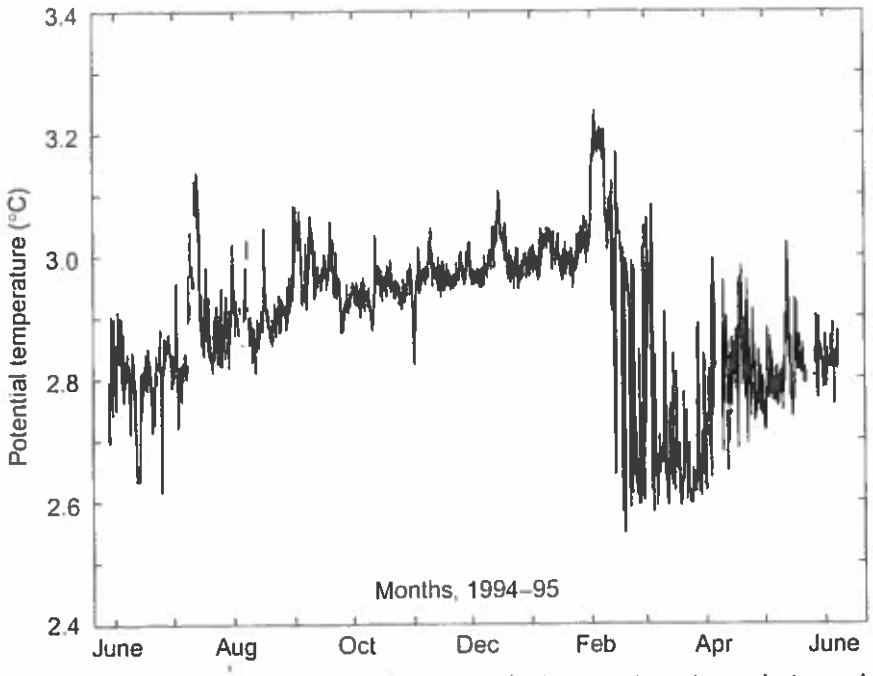

Fig. 5.5.7 A 1-year record of temperature at 510 m illustrating the increase in variance during and after the mixed layer reaches the depth of the instrument in early February 1995.

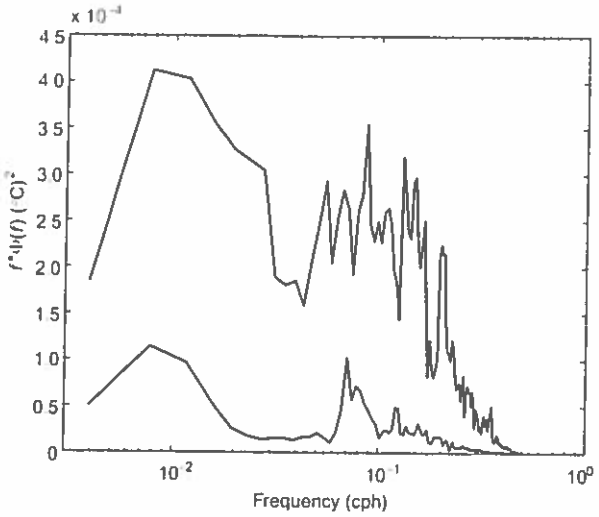

Fig. 5.5.8 Two variance-preserving spectra based on 2048 1-h blocks of data from the 510 m temperature record illustrated in Figure 5.5.7. The lower-energy block occurs between 30 September and 25 December 1994, before the mixed layer reaches the instrument. The more energetic block occurs between 8 March and 1 June 1995 during convection and after it ceases.

temperature versus salinity plots at four depths during 21 days in March when convection was at its full extent and the density at these levels was relatively constant in time (Fig. 5.5.5, see Plate 5.5.5, p. 428). At each depth the hourly observations show the extent of the fluctuations and the fact that they are largely parallel to the constant density surfaces.

The likely cause of the fluctuations (Lilly *et al.*, 1999) is that they are horizontal variations in temperature and salinity being swept past the mooring by the current. These authors showed that the necessary horizontal variability was indeed observed in data from P-ALACE float records. Recent work by Rudnick and Ferrari (1999) suggests that these compensating horizontal variations in temperature and salinity may be ubiquitous features of the mixed layer whether it is convecting or not. They carefully studied such variations in the upper mixed layer of the Pacific Ocean. Using data obtained from a Conductivity-Temperature-Depth (CTD) profiler towed over 10° of latitude at 50 ± 0.3 m the authors establish that horizontal gradients in temperature and salinity over scales of 20 to 10 000 m

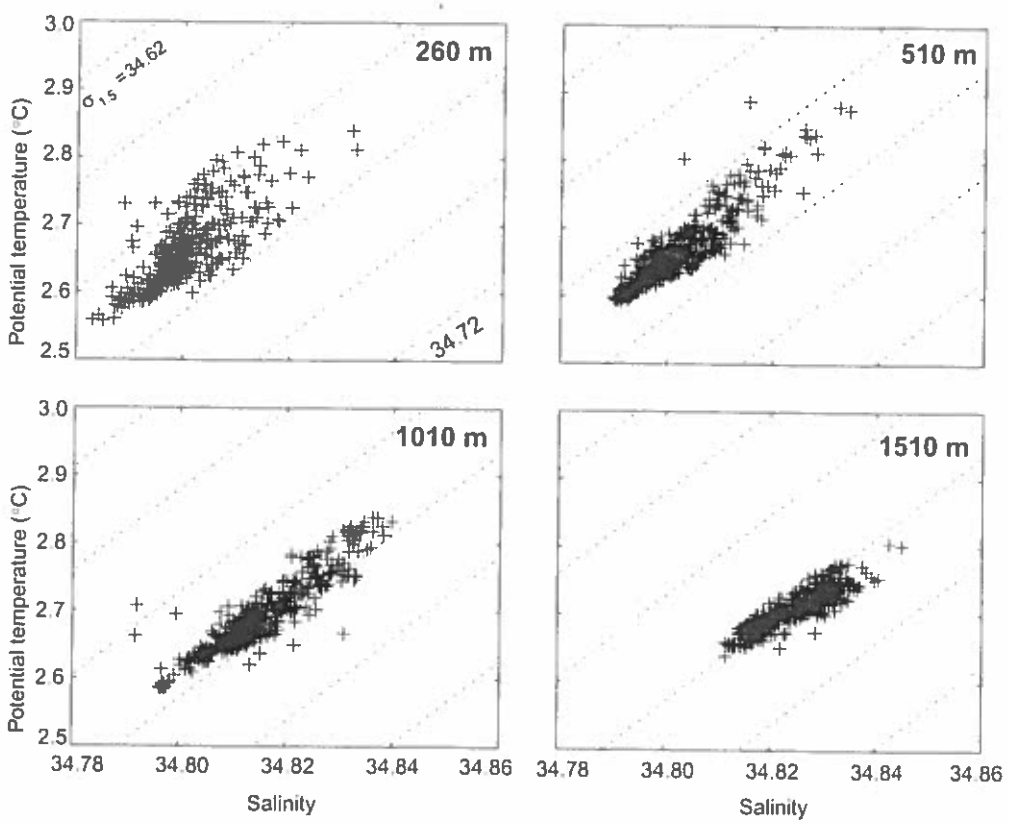

Fig. 5.5.9 Temperature versus salinity diagrams based on data obtained at 260, 510, 1010 and 1510 m, between 12 March and 2 April 1995, during the final stage of convection when the density at these depths remained relatively constant.

'tend to compensate in their effect on density'. From these results we tentatively conclude that the compensating temperature and salinity variations originate in the surface layer and are propagated to intermediate depths during convection.

Data equivalent to that obtained by Rudnick and Ferrari (1999) has not been collected in the Labrador Sea. However, CTD profiles collected in February and March 1997 suggest a similar situation exists there, even during deep convection. Temperature and salinity data collected in the upper 600 m at four locations, separated by 30 km, on 25–26 February and 8–11 March, are plotted in Figure 5.5.10 with similar symbols denoting similar locations. The range in $\sigma_{1.5}$ in both groups of stations is $\approx 0.01\,\mathrm{kg\,m^{-3}}$ while the temperature and salinity variations are 0.1°C and 0.02, respectively. In their effects on density the horizontal gradients in temperature largely compensate the gradients in salinity, just as observed by Rudnick and Ferrari (1999). Figure 5.5.10 also demonstrates that the magnitudes of the gradients remain roughly constant with time as the mixed layer deepens from 700 to 1100 m (Fig. 5.5.2). From this we conclude that the temperature and salinity gradients propagate down to intermediate depths, with the deepening mixed layer, where they are carried along in the current to be observed as fluctuations by moored instruments.

Currents at the Labrador Sea mooring are, according to Lilly *et al.* (1999), variable and predominantly barotropic. The variability in direction is readily apparent in the progressive vector plot of the 750 m record shown in Figure 5.5.11. Subsequent data from 5 years' deployment of the *Bravo* mooring show the Eulerian mean horizontal velocity at this site to be rather unpredictable from year to year. The speed of the flow is $\approx 0.15\,\mathrm{m\,s^{-1}}$ from the beginning of the record to the end of August and from the beginning of March to the end of the record. For the months of October through February the speed is $\approx 0.07\,\mathrm{m\,s^{-1}}$, or half the value over the other months. Neither these changes, nor the changes in direction seen in Figure 5.5.11, appear to be related to the arrival of the convection layer that reaches to the depth of the instrument throughout March. The large-scale flow, it seems, is not altered by the presence of convection. However, the study of eddies in the region by Lilly and Rhines (2000) shows that intense, sub-mesoscale and mesoscale eddies, overwhelmingly anticyclonic, populate this site. Kinks in the progressive vector diagram

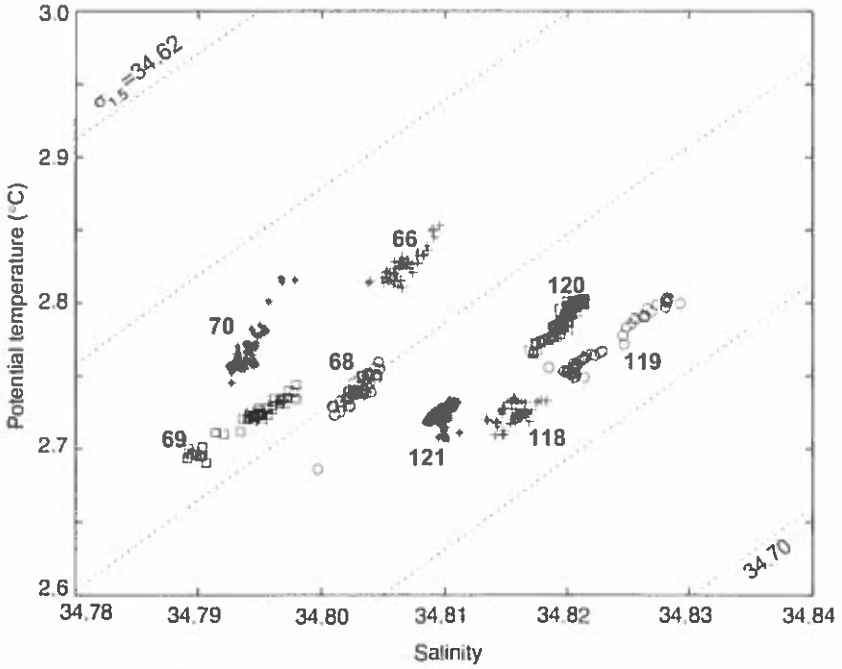

Fig. 5.5.10 Temperature and salinity values from the mixed layers of four pairs of RV *Knorr* CTD stations obtained in the mid-Labrador Sea during convection in early 1997. Stations 66 and 118 (56.8°N 54.2°W) were obtained on 25 February and 8 March; Stations 68 and 119 (57.0°N 53.9°W) on 25 February and 10 March; Stations 69 and 120 (57.3°N 53.7°W) on 26 February and 10 March; and Stations 70 and 121 (57.5°N 53.4°W) on 26 February and 11 March.

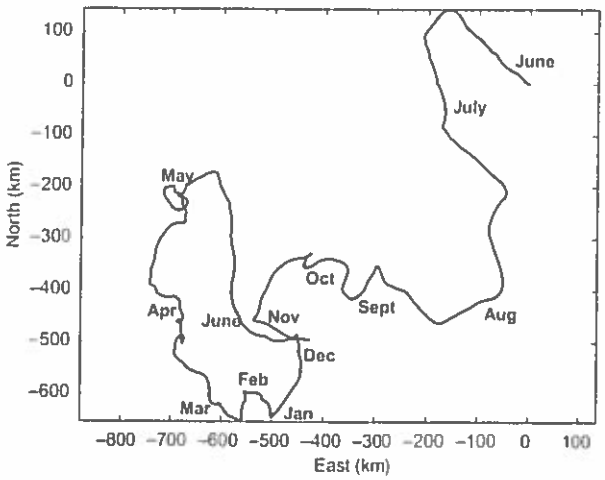

Fig. 5.5.11 Progressive vector diagram from hourly observations at 760 m on the *Bravo* mooring between 29 May 1994 and 13 June 1995. Labels indicate the first observation in each month.

correspond to passage of such eddies. In cold years, active with wintertime convection, many of these eddies have an identifiable core of relatively pure, cold, convected water and hence are associated with convection. Their origins are not yet known, but the dynamically active boundary currents on both Greenland and Labrador continental rises are two known sources, and their generation purely by convection has been documented in model studies (Jones and Marshall, 1993; Maxworthy and Narimousa, 1994; Rhines, 1998).

As noted, the speed of the current from October through February is $\approx 0.07\,\mathrm{m\,s^{-1}}$ and roughly twice that after 1 March. Long-lived sub-mesoscale and mesoscale eddies have, in subsequent years altered this simple picture of a late-winter maximum in kinetic energy. The first of the two pieces of data used to calculate the spectral estimates shown in Figure 5.5.8 is therefore in the slow regime, while the later one is in the fast regime. If horizontal gradients being swept past the mooring are the cause of the temperature and salinity variability in the moored records, the doubling of the current speed would cause a doubling of the frequency of features with fixed horizontal scales. This effect is not obvious between the two spectra because the horizontal scales of the gradients are distributed broadly over the spectrum. Thus no clearly defined spectral peaks are created to be traced from one period to another except possibly the peak in the early spectrum at ≈ 0.07 cph (cycles per hour). This broad peak includes two maxima; one at the inertial frequency (0.067 cph) and one for the semi-diurnal tides (0.08 cph) but it can't be identified in the later spectrum because of the large scatter.

When convection stops, the vertical density stratification is re-established and the horizontal gradients that were brought to intermediate depths in the mixed layer are no longer renewed. Those existing when convection ends are slowly mixed away by horizontal eddy diffusion. Assuming a horizontal scale L of 100 km for the region of convection with its small-scale horizontal variations, then the time scale of eddy mixing will be about L^2/K_H, where K_H, the horizontal eddy diffusivity, is $\approx 10^3\,\mathrm{m^2\,s^{-1}}$ (Sundermeyer and Price, 1998). This gives a time scale for the horizontal mixing of ≈ 4 months, which is about the decay time observed in the records.

5.5.4 Restratification

At the end of the cooling season, vertical mixing due to convection ceases and its dominant influence on mid-depth water properties ends. This also marks the beginning of the restratification process, during which the vertical stratification that existed prior to the homogenization is re-established. As mentioned earlier, the end of convection is indicated by the rapid decrease in $\sigma_{1.5}$ at 260 and 510 m over the first 20 days in April indicated in Figure 5.5.5 (see Plate 5.5.5, p. 428). There are no data for this year after early June 1995 but there is a decreasing trend in $\sigma_{1.5}$ at 260, 510 and 1010 m between June 1994 and the arrival of convection in February 1995. This, we assume, is due to a continuation of the restratification process following deep convection in the winter of 1993–94, which suggests to us that there are two restratification time scales: an initial rapid change that takes place over the month immediately after the cessation of convection, and a multimonth adjustment that continues until it is interrupted by the next convection event. Presumably a steady-state vertical density profile would eventually be reached if convection did not intervene.

Considering the initial stage of restratification evident in Figure 5.5.5 (see Plate 5.5.5, p. 428), it is not clear if this indicates an end to convection over a large area, or the advection of a stratified non-convecting water column to the observation site. However, the first option seems more likely as the end of convection appears in other records as a

rather rapid event marked by a rapid increase in stratification, especially in the upper layers. One of the best observations of restratification over a larger area was obtained from a tomographic array that integrates the water properties over the array to give a larger-scale picture than a single mooring can. This was obtained in the Golfe du Lion by Send *et al.* (1995), who found a period of restratification after the end of convection lasting ≈40 days. Another example is the salinity record from P-ALACE float 392 in the Labrador Sea (Davis, 1998a; see also Davis and Zenk, Chapter 3.2). This shows, in early 1996 and 1997 in the central Labrador Sea, a sudden transition between the low stratification associated with convection and a stratified water column. This record is admittedly like a mooring, from a single point, but it does give a consistent picture in the 2 years.

The restratification process has been modelled numerically by Jones and Marshall (1997), who envisage a homogeneous cylinder of water floating in an ocean of constant stratification. The density gradient between the cylinder and the surrounding ocean gives rise to a narrow cyclonic current that breaks up via baroclinic instability into baroclinic eddies. These horizontally mix the homogeneous water with the stratified waters, dissipating the homogeneous cylinder in time scale, τ. For the special case where the stratification in the water surrounding the homogeneous cylinder is concentrated in the upper layer, h,

$$\tau \approx 56 r/(h\Delta b)^{1/2}$$

where r is the radius of the homogeneous cylinder, h is the depth of the upper stratified water bounding the homogeneous cylinder and Δb is the difference in density between the homogeneous water and the surrounding water in buoyancy units. For the Labrador Sea where $h \approx 500$ m, $\Delta b \approx 2 \times 10^{-3}$ m s^{-2} and $r \approx 100$ km, $\tau \approx 65$ days. This result is about twice the 1-month time scale for the rapid restratification but one-fifth of the 10-month time scale for the slow restratification suggested in Figure 5.5.5 (see Plate 5.5.5, p. 428). This suggests the modelling result is more applicable to the rapid phase of restratification.

Additional evidence of the long period restratification has been obtained from CTD data collected in May and October of 1996. An example of the changes in isopycnal depth during this 5-month interval is shown in Figure 5.5.12, in which are plotted the depths of four isopycnals across the Labrador Sea during the two cruises. At the stations between 400 and 600 km the isopycnal depths increase significantly between May and October, while the 27.72 and 27.74 kg m^{-3} surfaces between 650 and 790 km show a decrease in depth. Vertical profiles from this data set, presented in Figure 5.5.13, illustrate a different aspect of the same phenomenon. The solid curves in this figure are from the May cruise, the shallowest four from between 400 and 600 km and the deeper three from 650 to 790 km. October profiles from the same locations are dotted. As in Figure 5.5.12, the shallower isopycnal surfaces between 400 and 600 km descend, during the 5 months between cruises, while the deeper surfaces between 650 and 800 km rise.

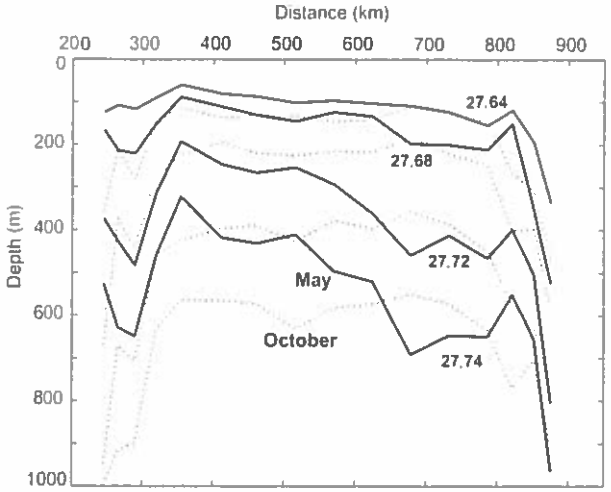

Fig. 5.5.12 Four surfaces of constant σ_0 (potential density anomaly relative to 0 m) across the Labrador Sea based on CTD data collected in May 1996 (solid lines) and October 1996 (dotted lines).

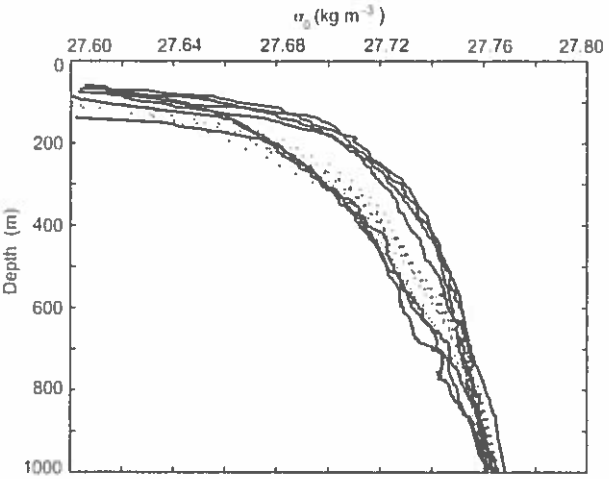

Fig. 5.5.13 Vertical profiles of σ_0 across the Labrador Sea in May (solid) and October 1996 (dotted).

The region between 400 and 600 km region is where convection has been observed to reach its greatest depth in winter. This was most recently observed during the February 1997 *Knorr* survey of the Labrador Sea, when the deepest mixed layer along the CTD line across the Labrador Sea, shown in Figure 5.5.1, was 1100 m at the 3000 m isobath on the Labrador side, 700 m in the centre of the basin, and 200 m at the 3000 m isobath on the Greenland side (Lab Sea Group, 1998, Fig. 16). These observed isopycnal depth changes reflect a slow adjustment following convection. Lighter water, from beyond the region of deepest convection, moves into the upper water column in the region of deepest convection, while denser water in the region of deepest convection moves outward at mid-depth. Eddy diffusion appears to be the primary reason for these changes.

Another view of restratification is obtained in the temperature and salinity time series obtained on a mooring over the 1994–95 winter in the middle of the Labrador Sea. When these values are plotted against each other as in Figure 5.5.14, it is clear that temperature and salinity at these depths slowly increase between periods of convection and that density slowly decreases. The decrease in density is the same decrease observed in the two previous figures while the temperature and salinity increases are signatures of the Irminger Water invading the central region.

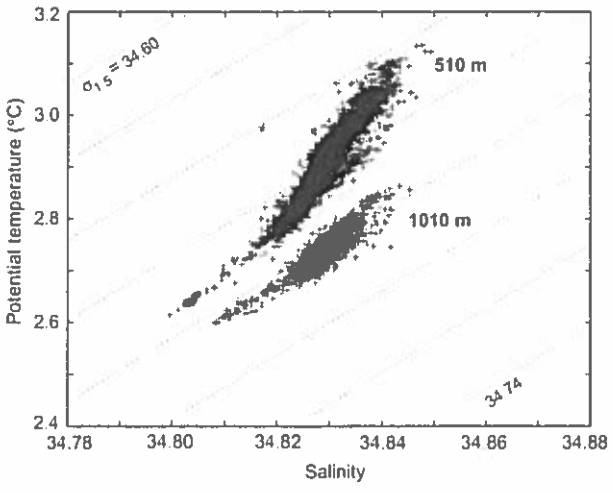

Fig. 5.5.14 Temperature versus salinity at 510 and 1010 m from the *Bravo* mooring during the period of restratification between June 1994 and January 1995, i.e. before the mixed layer reached these sensors in February 1995.

5.5.5 Summary and discussion

Our purpose in this chapter has been to present a short review of deep convection concentrating on advances made during the WOCE observing period. Using mostly examples from the Labrador Sea we began with a discussion of the depth, homogeneity and energy changes of the deepening mixed layer, as well as some interactions between the mixed layer and the underlying stratified water based on observations obtained during the winter of 1997. Data obtained in July 1993, following a series of severe winters, demonstrated that the convectively mixed water (Labrador Sea Water) represents ≈40% of the cross-sectional area of the deep Labrador Sea and is the dominant water mass of the region. The work of Sy *et al.* (1997) demonstrated the flow of this water away from the Labrador Sea at intermediate depths toward the east to be more rapid than previously thought and the work of Curry *et al.* (1998) revealed a 5-year delay between the volume of LSW in the Labrador Sea and water properties at intermediate water in the subtropical gyre.

Details of convecting plumes such as their diameter (≈1 km), rate of descent (maximum ≈0.13 m s^{-1}, mean ≈0.02 m s^{-1}), rotation (not yet resolved), and the net downward mass flux in a convecting region (≈0) were presented following the work of Schott *et al.* (1993b, 1996). The ideas of Lilly *et al.* (1999) with respect to the increase in temperature and salinity variability observed at mid-depth during and following convection in moored time series records was revisited with the addition of the work of Rudnick and Ferrari (1999). Their work suggests that density-compensating temperature and salinity gradients are ubiquitous in the mixed layer, which led us to suggest that the observed increased variability is due to these pre-existing gradients being swept past the sensors after they have been propagated to intermediate depths by deep convection.

Our discussion of restratification following convection suggested a two-stage process. First is a rapid change lasting a month or so, possibly related to baroclinic eddies generated from baroclinic instability in a current at the edge of the convecting region, as suggested by Jones and Marshall (1997). The second stage, a multi-month process, involves the slow decrease in the mixed water as it flows away from the region and its replacement at

lower densities by water inflowing from the boundaries.

While the focus of this chapter has been on the Labrador Sea, numerous aspects of the convective processes discussed here apply as well to the other two locations of open-ocean convection in the North Atlantic: the Greenland Sea and the Mediterranean Sea. For example, all three regions are subject to strong wintertime winds blowing off the adjacent continental boundaries. These seasonal winds bring cold, dry air over the relatively warm ocean (the air–sea temperature contrast is especially large in the Mediterranean Sea), leading to the high buoyancy loss that drives the overturning. A second common factor among the regions is the 'layering' of *in-situ* water masses within the water column. Each sea is characterized by a relatively cold and fresh upper layer, warmer and saltier water beneath this, and a larger body of weakly stratified water occupying the middle of the water column (i.e. the remnant of the convective product from earlier years). The relative volumes and properties of these layers can modulate the occurrence of convection. For example, a large abundance of water remaining from an earlier period of convection predisposes the water column to further overturning. On the other hand, enhanced flux of the highly buoyant surface water to the convection region can help inhibit the overturning. This effect appeared to be important during the late 1960s when the Great Salinity Anomaly invaded the Labrador Sea (Lazier, 1980).

A third important similarity between the three areas of convection is the regional circulation; each of them is characterized by a cyclonic flow regime. This is undoubtedly a crucial aspect of the preconditioning for convection. The isopycnal doming in the centre of each of the 'gyres' allows the more weakly stratified subsurface waters to reside closer to the sea surface and hence be more readily subject to the atmospheric buoyancy forcing. Furthermore, in each sea, part of the cyclonic flow regime involves boundary currents (e.g. in the Mediterranean Sea it is the westward flowing Northern Mediterranean Current). This has several ramifications. It enhances the ability for newly formed water masses to exit the region, and influences the restratification process since the boundary currents contain more highly stratified water. Additionally, there is increasing evidence that convection may at times occur directly within the boundary currents (Mauritzen, 1996a; Schott *et al.*, 1996; Pickart *et al.*, 2000a), since after all this is where the heat loss is greatest.

But as there are common threads to the overturning in the Labrador, Greenland, and Mediterranean Seas, there are also significant regional differences. The Greenland Sea is unique in that ice plays a significant role in the preconditioning phase. As discussed in Marshall and Schott (1999), the deepest overturning occurs in late-winter just after the ice-free 'Nord Bukta' region opens up. In the Mediterranean the winds are more localized in space than in the other two regions (Candela, Chapter 5.7). This clearly impacts the convection, as the region of deepest mixed layers generally lies in the path of the Mistral winds. Furthermore, these winds are not cold enough to cause convection during daylight hours, so the Mediterranean has a daily cycle of overturning that is not present in the other two seas. Also, the impact of the basin-scale NAO wind pattern impacts the Labrador and Greenland Seas to a much greater extent than it does the Mediterranean. Finally, the respective sizes of the convection zones and convected water masses differ greatly. In the Mediterranean, the convecting patch is of order 50 km wide; in the Greenland Sea it is of order 100 km wide; and in the Labrador Sea the zone of convection approaches 500 km width, and includes the boundary currents.

Convection at each of these three Atlantic sites contributes to the global meridional overturning circulation, although the quantitative measures are not yet known. In the Greenland Sea particularly, the deep convection into the cyclonic gyre seems rather isolated from the processes that produce the dense overflows (Mauritzen, 1996a). Mediterranean water and Labrador Sea water both make an obvious contribution to the Upper North Atlantic Deep Water, respectively, as very high- and low-salinity end points. Distant identification of Labrador Sea Water follows its low salinity, potential vorticity, and low nutrient concentration, high dissolved oxygen, tritium and CFCs. The rate of efflux of Labrador Sea Water into the open Atlantic is known to vary greatly, with the intensity of wintertime forcing. Johns *et al.* (1997a) observe velocity and CFC maxima associated with both deep and shallow NADW near Abaco, some 5000 km south of the Labrador Sea. A striking increase in CFCs (even after adjusting for time-dependence of the

source) was seen in 1995–96, subsequent to the intensely cold winters of 1988–94, and before this a path change was observed by their current meter array. The 8- to 10-year transit time is slower than the core-current speeds would suggest, yet faster than earlier estimates. For the era ending 1977, Jenkins and Rhines (1980) observed dilution of the tritium maxima of the deep western boundary currents by factors of order 10, from the subpolar gyre to the Blake–Bahama Outer Ridge; this indicated dilution and delay (by recirculation) mechanisms *en route*, which were later explored in model studies by Pickart (1988).

Model studies (Hallberg and Rhines, 1996) suggest that when convection is initiated or increased at the high-latitude source, a pressure wave propagates down the western boundary, as a topographic Rossby wave, well before the arrival of tracer-tainted, identifiable water mass. Such model studies (also that of Winton, 1997, and Spall and Pickart, 2000) point out that sloping continental rise topography acts as a waveguide, and rather gently leads dense water masses equatorward from high latitude, as they gently sink. Thus, 'sinking' is minimal in the near-field of the convection, but occurs downstream. Production of kinetic energy of the overturning circulation by potential energy created by buoyancy forcing requires that dense water sink and less dense water rise, but the sites of sinking and rising are, at least in model studies, often distant from the convection. In a diapycnal/epipycnal coordinate system, however, convection is more locally associated with time-averaged diapycnal transport ('water mass conversion'). Such analyses are beginning to be carried out with models and are an insightful way to approach the link between convection, sinking and global meridional overturning.

Thus we are still seeking to quantify production rates of the constituent water masses of the global meridional overturning. Outward transport of Labrador Sea Water is even difficult to define, because of extensive recirculation within the sub-polar gyre and entrainment once the water mass has left the subpolar gyre. Estimates have ranged from less than 1 Sv to more than 10 Sv. By using the relaxation rate of the central Labrador Sea Water after cessation of convection (either annually or, through periods of negative NAO index, interannually), we estimate that renewal of that mass occurs at a rate that decreases with depth from the surface and residence times ranging from roughly 2 years above, to greater than 5 years at 2000 m (Lilly *et al.*, 1999). Much remains unknown about the detailed geography of deep convection and circulation. In the Labrador Sea, both interior and boundary currents are known to participate in the deep convection (Spall and Pickart, 2000, estimate 1–2 Sv of boundary current production). The boundary current, however, is shielded from deep convection by low-salinity shelf waters at some sites. Where the circulation crosses from Greenland to Labrador, the boundary currents broaden and slow, and are generally exposed to some of the most intense air–sea heat flux in the Sea; here and over the wide continental slope near Labrador, convection may be particularly deep (Cuny *et al.*, 2000).

Direct velocity and transport measurements are needed to augment water mass observations. Unfortunately the Lagrangian movement of water masses is difficult to observe, even with modern 'quasi-Lagrangian' floats and drifters. Lavender *et al.* (2000c) describe the Labrador/Irminger Sea circulation as observed with P-ALACE floats. They concentrate on the Eulerian ensemble mean velocity field, and remark that 'no floats travelled southward to the subtropical gyre in the deep western boundary current, the putative main pathway of dense water in the meridional overturning circulation.' If the boundary current is concentrated to a narrow width, for example at the Flemish Cap, then these profiling floats may have difficulty staying within it; tracer observations assure us that the transport does take place.